Self-Assembly of Nanoparticle Arrays on Semiconductor Substrate for Charge Transfer Cascade†

Gilad Gotesman,‡ David H. Waldeck,§ and Ron Naaman*,‡

Department of Chemical Physics The Weizmann Institute of Science, Rehovot 76100, Israel, and Department of Chemistry, University of Pittsburgh, Pittsburgh, Pennsylvania 15260

Received: October 6, 2008; Revised Manuscript Received: November 22, 2008

The current study focuses on the interaction between hierarchical structures of nanoparticles (NPs) and a semiconductor substrate on which they are assembled. Monolayer and bilayer assemblies of two different NPs were prepared on the surface of a GaAs substrate. The photoluminescence response of the bilayer assemblies depends on their hierarchy, namely on the ordering of differently sized nanoparticles with respect to the surface; however, the surface photovoltage does not. Based on these studies, it is possible to determine the importance of each of the possible quenching mechanisms for electron−hole pair excitation.

Introduction

The idea to use semiconductor nanoparticles (NPs) for solar energy harvesting and photovoltaic applications has sparked intensive research into the nature of light induced charge transfer between NPs and between NPs and various substrates.[1−6] One may envision that a device based on NPs will contain NPs of various band gaps, so as to cover most efficiently the solar spectrum, and that these NPs will self-assemble into a robust superstructure. For such structures one would like to direct the course of charge transfer and to optimize the parameters affecting its yield.

In recent studies, NPs were assembled in multilayer structures applying the Langmuir−Blodgett technique,[7] layer by layer (LBL) assembly[8,9] or self-assembly methods and their luminescence properties were investigated.[10] Electronic energy transfer has been studied between NPs of the same type,[11−13] or between NPs made from different materials either when the particles are deposited as thin films or when they are assembled together through chemical or electrostatic interactions.[14,15]

This work studies hierarchical superstructures that are composed of semiconductor NPs linked by organic molecules to a semiconductor substrate. The assemblies contain up to two layers of NPs and are built from two different NP sizes. This system provides a model for light harvesting NP arrays that might be used in photovoltaic applications for providing vectorial charge transfer from the excited NPs to the substrate. In such assemblies nonradiative quenching of photoexcited electron−hole pairs can occur by energy transfer[9−13] or charge transfer.[4,14,15] An energy transfer process based on dipole−dipole interactions depends on the distance between the donor and the acceptor and allows the energy transfer from larger to smaller bandgap materials. Other than distance, it is weakly dependent on the nature of the linker that binds the donor and acceptor.

In the case of quenching by charge transfer, the mechanism is based on tunneling of electrons, holes or both and the rates depend strongly on the electronic nature of the "bridge" molecule that links the donor and acceptor. Although net charge transfer in the assemblies can be detected by changes in the workfunction of the systems, photoluminescence (PL) measurements are sensitive to both charge and energy transfer.

In the present study, we show that the PL signal from the NPs in these assemblies depends on their order, i.e., placement of the two different NPs relative to the substrate and on the interaction with the substrate. We also show that the photovoltage in the assemblies is increased over that for the bulk electrode and that the contributions from the different NP layers are roughly additive, with a minor dependence on the NP order. By combining PL and contact potential difference (workfunction) measurements, we are able to distinguish the contribution of the energy transfer quenching from that of the net charge transfer.

Materials and Methods

The preparation of the GaAs-NPs assemblies was based on the self-assembly of the NPs on a GaAs substrate via a self-assembled monolayer (SAM) of dithiol molecules that serve as the linker between the NPs and the substrate. The semiconductor NPs used were core-only CdSe nanoparticles (Evident Tech.) with average diameters of 2.7 and 6.8 nm ("small" and "large" NPs respectively) and "band gaps" of 2.4 and 2.0 eV, respectively (see Supporting Information for absorption and emission spectra of these NPs solutions). Figure 1 outlines the principles of the sample preparation and presents scanning electron microscope images of the results at each stage of preparation. A detailed description of the preparation and characterization is provided in the Supporting Information. Either 1,9-nonanedithiol (DT) or 1,4-benzenedimethanethiol (BDT) molecules were used to link between the two NPs layers. The DT molecules were adsorbed on the GaAs by applying the procedure described in ref 16 and the resulting monolayers were characterized by ellipsometry (Figure 1A). The samples were then immersed in a solution containing the NPs to adsorb the first NPs layer (Figure 1B). Next, the bifunctional linker molecules were adsorbed on the NPs layer (Figure 1C) followed by immersion in a different NPs solution to adsorb the second NPs layer (Figure 1D).

Parts E−G of Figure 1 show high resolution scanning electron microscope images of the "large on small" NPs assembly at different stages of this "bottom up" procedure; the same principles were applied to assemble the "small on large" system.

† Part of the "Robert Benny Gerber Festschrift".

* Corresponding author. E-mail: ron.naaman@weizmann.ac.il.
‡ The Weizmann Institute of Science.
§ University of Pittsburgh.

10.1021/jp808803v CCC: $40.75
Published on Web 01/09/2009

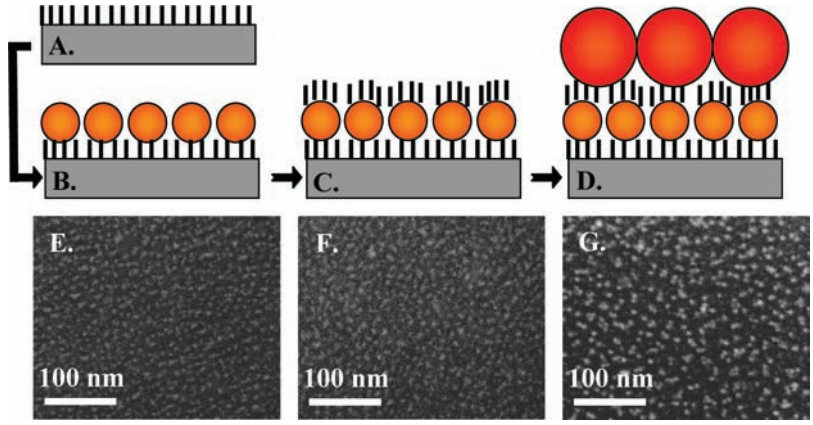

Figure 1. Adsorption scheme and SEM images for the four steps of the bilayer-NPs-system assembly (large NPs on DT on small NPs in this case): (A) adsorption of DT monolayer on GaAs substrate, (B, E) adsorption of the first NP layer, (C, F) adsorption of the linker molecule, and (D, G) adsorption of the second NP layer.

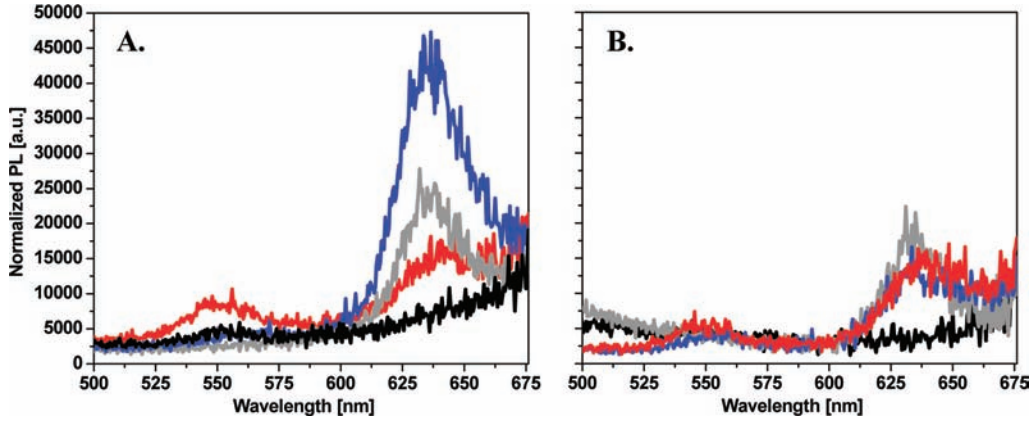

Figure 2. PL spectra of: small NPs (black), large NPs (gray), large NPs on small NPs (blue) and small NPs on large NPs (red) layers on *p*-type GaAs substrate with DT linker molecules. (A) Measurements right after adsorption and (B) measurements 1.5 months after adsorption (the samples were kept in plastic tubes at ambient atmosphere). Excitation was at 350 nm.

A very dense and uniform monolayer of small CdSe NPs was formed (see Figure 1E) with a coverage of about 8.7×10^{11} particles/cm.^{2} Albeit larger, this coverage is similar to that found when large NPs are used for the first layer, about 5.5×10^{11} particles/cm^2. Figure 1G shows the case in which large CdSe NPs have been adsorbed to a dithiol layer on top of the layer of small NPs. The brighter spots in this figure are assigned to the large NPs and their coverage is lower than that of the underlying layer of small NPs, approximately 4×10^{11} particles/cm^2, and of the large NPs in the single layer case. When a sample with a monolayer of small NPs was dipped into a solution of large NPs, without adsorbing the linker molecule first, only a very small amount of large NPs could be found on the sample, as compared to the situation with the linker molecules (see Supporting Information). This control experiment indicates that chemical binding between the two differently sized NPs, via the second exposure to linker molecules, occurs. There is no direct evidence that the NPs of the second layer are placed exactly vertically on top of NPs in the first layer. Because the first layer is dense enough and the second NPs layer is chemically bound by the organic linker to the first one, the assembly can be approximated by the scheme shown in Figure 1D.

A combination of photoluminescence (PL), contact potential difference (CPD) and surface photovoltage (SPV) studies were used to characterize the assemblies. Wavelength resolved PL measurements (Fluorolog-3 Spectrofluorometer, Horiba Jobin Yvon, France) were performed at room temperature. CPD and SPV studies (Delta Phi Besocke, Jülich, Germany) were performed to probe the variation of the workfunction of the GaAs substrate upon adsorption of the NPs, in the dark and upon illumination, respectively.[17] The change in the assembly's workfunction correlates with net charge being transferred between the substrate and the NPs. Three different sets of samples were investigated and the results presented are averages of these three trials.

Results and Discussion

Figure 2 shows PL spectra of different NP assemblies on a *p*-type GaAs substrate, using the DT molecules as linkers. The assemblies were illuminated by 350 nm light (3.5 eV) so that both types of NPs as well as the GaAs substrate are excited. The emission from the substrate is responsible for the rise of the signal toward the red. The scheme at the bottom of Figure 3 illustrates the structural motifs of the six systems that were studied: (1) small NPs layer, (2) large NPs layer, (3) large NPs with DT linker on top of a layer of small NPs, (4) small NPs attached with a DT linker onto a layer of large NPs, (5) large NPs attached via BDT linker on top of a layer of small NPs, and (6) small NPs attached via a BDT linker on top of the large NPs layer. The emission from the small NPs was peaked at ~550 nm and that from the large NPs at ~636 nm. Figure 2A shows that the intensity ratio of the PL emission from the small and large NPs changes as their proximity to the substrate changes. The existence of the substrate introduces an asymmetry in the NPs relative PL yield; i.e., the bilayer assemblies have

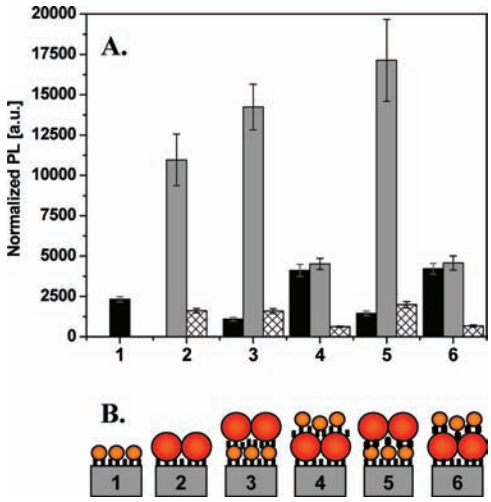

Figure 3. (A) Average peak photoluminescence intensity of the different NP-systems on *p*-type GaAs, when exciting both NPs (small NPs in black, large NPs in gray) at 350 nm and when exciting only the large ones (crossed white) at 560 nm. (B) Scheme of the different NPs-systems: (1) small NPs, (2) large NPs, (3) large NPs on DT on small NPs, (4) small NPs on DT on large NPs, (5) large NPs on BDT on small NPs, (6) small NPs on BDT on large NPs.

different emission intensities for the NPs. Because the GaAs substrate is known to be easily oxidized,[16,18] additional measurements of the same samples were made 1.5 months after their exposure to the air (Figure 2B). No baseline subtraction was performed in all the spectra shown.

When the samples were left to oxidize, the relative position of the two types of NPs to the substrate does not affect their emission yield. The oxidized bilayer system becomes symmetric, namely the relative emission is the same when the small NPs are on top of the large ones or vice versa. Hence, no dependence of the emission yield on the hierarchy of the assembly is found. In addition, all the experiments were repeated with *n*-type GaAs (see Supporting Information) and the obtained results are similar to that obtained with the *p*-type substrate.

Figure 3 shows a more quantitative comparison of the PL data for the different assemblies: different bilayer structures and different organic linkers. To compare quantitatively the signals from the different structures, spectra were taken within an interval of 40 nm around the peak position with a longer integration time to improve the signal-to-noise ratio, and the signal at the peak was averaged for three different sets of samples. The data were normalized for the incident photon flux, and the PL signal from the GaAs substrate, coated with a SAM of DT, was subtracted from the observed signals. PL studies were performed with 350 nm excitation (3.54 eV) and with 560 nm (2.21 eV) excitation. Photons at 2.21 eV can excite the large NPs and the p-type GaAs substrate but are not able to excite the small NPs. The 3.54 eV photons excite all three components of the assembly: large NPs, small NPs and the GaAs substrate.

For all cases, when bilayers of particles are probed (samples 3, 5 and 4, 6), the particles that are on top emit more efficiently as compared to the case when the same particles are adsorbed as a single layer (samples 1 and 2, respectively). This increase occurs despite the fact that the coverage of the top NPs layer is lower than the coverage of a single layer. This result can be explained by the longer distance between the top layer of NPs and the substrate, relative to the single layer case. Because the GaAs substrate band gap is narrower than that of the particles, and because the density of states in the substrate is much larger than that of the NPs, the substrate is an efficient acceptor both for energy and for charge. Both of these quenching mechanisms decrease strongly with the distance from the substrate.[19,20] In addition, the data show that the bottom layer of NPs in the bilayer systems (3, 5 and 4, 6) are quenched more efficiently than in the case of a single layer (1 and 2, respectively).

The addition of a second layer of thiols on top of the bottom layer of NPs creates an additional quenching pathway (see Supporting Information). This effect can account for most of the quenching of the large NPs in the sandwich layer but only accounts for about half of the quenching observed for the small NPs in the sandwiched layer. The additional quenching for the small NPs in the sandwiched layer is attributed to energy transfer to the large NPs in the top layer. Namely, in the case of bilayers with small NPs in proximity to the substrate, the PL is quenched both by the substrate and by the top layer of large NPs. The overall luminescence efficiency of the small NPs is reduced, as compared to the case when the small NPs are located on the outermost layer. The same behavior is observed for the BDT linker.

The data show that if only the large NPs are excited, the signal is lower, but the trends in emission yield are similar to that seen for the excitation at 350 nm. The PL signal depends on the hierarchy of the assembly.

Figure 4 presents results obtained from the CPD and SPV measurements, which are directly sensitive to net charge transfer between the substrate and the adsorbed NPs. The measurements were performed on fresh samples (Figure 4A) and on oxidized samples (Figure 4B) under a N_2 atmosphere. Each system was measured in the dark and under illumination at 410 nm (both NPs and substrate are excited) and 610 nm (only the large NPs and the substrate are excited). The data were collected after the signal had stabilized and the systems reached a steady state. The signal from GaAs coated with a monolayer of DT was subtracted from each measurement. Therefore, the presented change in the workfunction signal reflects the effect of the adsorbed NPs.

The dark measurements indicate that upon adsorption of the NPs the workfunction of the system decreased, as compared to the GaAs substrate coated DT SAM with no NPs. This decrease results from charge rearrangement in the system. The decrease in the workfunction indicates that when the first layer of NPs is adsorbed, electrons are transferred from the NPs to the substrate. Assuming a dielectric constant of 3 for the organic linker and a distance of about 1.6 nm (DT nominal length) between the NPs and the substrate, we estimate (by a simplistic model of a two plate capacitor) that an average charge of about 0.2e was transferred to the substrate per NP. Within the accuracy of the measurements, it seems that the amount of transferred charge is similar for the different assemblies in Figure 4A; however, the bilayers with small NPs on the outer layer show a somewhat smaller workfunction shift. When the assemblies are allowed to oxidize (Figure 4B), one finds almost no work function change for the single layer of NPs (relative to GaAs coated with DT SAM), and an increase in the work function for the NPs bilayers, independent of the order of the NPs layers.

Illumination of the assemblies induces a photovoltage that depends on the type of NPs and on the wavelength of the light. Both the 410 nm excitation and the 610 nm excitation are above the bandgap of the GaAs substrate, and the DT coated substrate displays a photovoltage (band bending) of about 280 mV. The photovoltage data shown in Figure 4C have this background contribution subtracted, and these values correspond to the photovoltage contribution from the NPs layers. The assemblies with large NPs (2−6) cause a significant increase in the

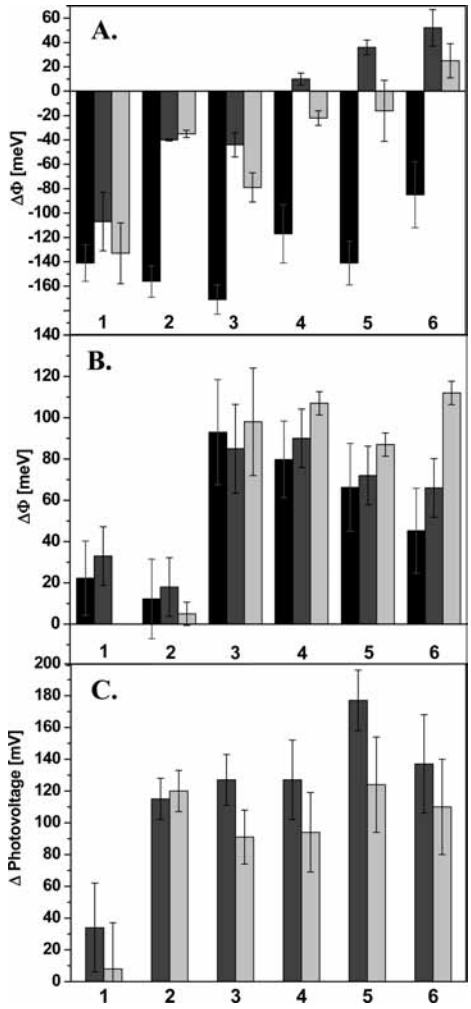

Figure 4. CPD and SPV signals from each NP assembly: in the dark (black), when exciting both NPs and the substrate at 410 nm (dark gray), and when exciting only the large NPs and the substrate at 610 nm (light gray). Panel A shows data for fresh samples and panel B shows data for oxidized samples. Panel C shows photovoltage data (relative to GaAs covered with DT; i.e. light−dark in panel A) of the fresh NP assemblies

SCHEME 1

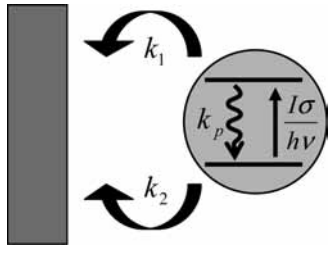

photovoltage whereas the small NPs (1) have a much more modest change. Also, the photovoltage of the bilayer assemblies shows a pronounced dependence on the wavelength, with 410 nm excitation giving rise to a systematically larger photovoltage than the same assembly excited with 610 nm light. In addition, the use of BDT as a linker between the NP layers, causes a photovoltage change that is systematically larger than that found with the DT linker.

Scheme 1 shows a simplified model that describes the photovoltage behavior of these assemblies for the simple case of a single NPs layer above the substrate. The four quantities in this diagram are the rate of electron−hole pair generation ($I \times \sigma/(h\nu)$), where I is the intensity, σ is the NP absorption cross-section and $h\nu$ is the photon energy), the recombination rate constant for the electron−hole pair in the nanoparticle (k_p), the rate constant for electron transfer to the substrate (k_1), and the rate constant for hole transfer to the substrate (k_2). The solution to this kinetic is given in the Supporting Information section. In the steady-state limit, we find that the population difference between the electrons and holes, $\Delta = n_p - h_p$, is given by

$$\Delta = \frac{k_2 - k_1}{2k_p}\left[\sqrt{\frac{4I\sigma \cdot k_p}{h\nu \cdot k_1 k_2} + 1} - 1\right]$$

when n_p and h_p are the electron and hole concentrations, respectively.

From this expression we see that the population difference scales as the square root of the light intensity. This finding is consistent with the experimental observation that for higher light intensities the photovoltage increases weakly with increasing light intensity. Note that the photovoltage experiments were performed at different intensities and the values reported in Figure 4 correspond to intensities where the photovoltage is only weakly changing with intensity (near saturation).

The SPV studies of the single NPs layers show that the small NPs display very little photoinduced charge transfer whereas the large NPs display a significant photovoltage. The average photovoltage, presented in Figure 4C, was calculated from Figure 4A by taking the difference between the black bar and the colored bar (dark gray for 410 nm excitation and light gray for 610 nm excitation). For the 410 nm excitation, one finds a 34 mV average photovoltage for a layer of small NPs (1) and a 115 mV average photovoltage for a layer of large NPs (2). In the case of 610 nm excitation, which is below the bandgap of the small NPs, almost no photovoltage is found for the small NPs and the large NPs present about the same photovoltage (120 mV) as in the case of 410 nm excitation. In the context of the kinetic model (Scheme 1) $k_2 > k_1$ for both systems, but the inequality is significantly higher for the case of the large NPs. Hence the photoinduced hole transfer is faster than the photoinduced electron transfer; namely, electrons are transferred from the substrate to the HOMO of the NPs more efficiently than they are transferred from the LUMO of the NPs to the substrate.

It is important to realize that the model does not include the case for which the substrate is excited and the NPs remain in the ground state. In this case, electrons from the substrate may be transferred to the LUMO of the NPs, charging it slightly negative. The indication that this process is not very important comes from the wavelength dependence of the SPV. This process should not depend strongly on the excitation wavelengths of 410 and 610 nm because they are both well above the GaAs bandgap. In contrast, the SPV results show a wavelength dependence, i.e., no photovoltage for small NPs at 610 nm illumination.

Although it is possible to extend the kinetic scheme to NPs bilayers, it becomes less useful unless numerical values are available for some of the rates. Instead, we provide a qualitative explanation for the observations. The photovoltage for assemblies 3 and 4 under 610 nm illumination is systematically lower than that of a single layer of large NPs and under 410 nm illumination is similar to that of a single layer of large NPs. The decrease in the photovoltage under 610 nm illumination can be explained by the increase in nonradiative recombination (increase in k_p in Scheme 1) that occurs when the second dithiol layer is placed on the large NPs (see discussion of PL). Under the steady state conditions used here, the magnitude of the effect

does not appear to depend on the hierarchy of the bilayer. Under 410 nm excitation both the small NPs and the large NPs in the bilayer are excited and this causes a slight increase in the photovoltage for cases 3 and 4. This increase is about the same magnitude as the value observed for case 1, a single layer of small NPs.

From Figure 4C it is evident that photoinduced charge transfer occurs mainly when the system includes the large NPs. When saturated alkanethiols are used to link the two NPs, the charge transfer between the NPs and the substrate does not depend on the order of the NPs. Namely, the charge transfer between the large NPs and the substrate is efficient even if the small NPs are sandwiched in between. When BDT is used to link the two layers of NPs, the photovoltage for case 5 is significantly larger than that for the saturated linker, but the increase for case 6 is similar to the case with the saturated linker. An enhancement of the charge transfer is expected for a conjugated bridge.[21] Apparently, this rate difference is important when the large NPs (which contribute most to the photovoltage) are in the outer layer but not so significant when they are in the inner layer.

The observations given here indicate that the photovoltage does not depend on the assembly's hierarchy but the photoluminescence yield does depend on the hierarchy. The photoluminescence yield is, in principle, a result of all the decay mechanisms, namely both energy transfer and charge transfer. Because the results indicate that the total PL yields depend on the order of the NPs, and because we have established that the charge transfer process does not depend on the order of the NPs, we conclude that the energy transfer process does depend on the proximity of the NPs to the substrate.

In the present work, scanning electron microscopy was used to show that it is possible to create assemblies of two differently sized NPs in a controlled manner, so that either the large particles are on the outermost layer or the small particles are on the outermost layer. The PL studies showed that the emission yield depends on the bilayer hierarchy in a predictable manner. In contrast, the photovoltage does not depend on the bilayer's hierarchy but does depend on the number of layers and on the nature of the linking molecules. Studies with both blue and red light excitation show that the contributions of each of the NPs layers to the total photovoltage are roughly additive. These findings suggest that the assembly of NPs multilayers could be used to enhance the photovoltage of a photovoltaic device, without being highly reliant on the NPs bandgaps or location in the assembly.

Acknowledgment. This work was partially supported by the US-DOE (Grant # ER46430), by the Israel Ministry of Science and by the Alternative Sustainable Energy Research Initiative of the Weizmann Institute. The electron microscopy studies were conducted at the Irving and Cherna Moskowitz Center for Nano and Bio-Nano Imaging at the Weizmann Institute of Science.

Supporting Information Available: Experimental procedures, absorption/emission spectra of the NPs solutions, SEM characterization of the NP assemblies, PL data of the NP assemblies with BDT linker, and PL, CPD and SPV data of the NP assemblies on *n*-GaAs. This material is available free of charge via the Internet at http://pubs.acs.org.

References and Notes

(1) Zhang, J. Z. *J. Phys. Chem. B* **2000**, *104*, 7239.
(2) Guldi, D. M.; Zilbermann, I.; Anderson, G.; Kotov, N. A.; Tagmatarchis, N.; Prato, M. *J. Mater. Chem.* **2005**, *15*, 114.
(3) S.Kang, M.; Yasuda, H.; Miyasaka, H.; Hayashi, M.; Kawasaki, T.; Umeyama, Y.; Matano, K.; Yoshida, S.; Isoda, H. I. *Chem. Sus. Chem.* **2008**, *1*, 254.
(4) Robel, I.; Subramanian, V.; Kuno, M.; Kamat, P. V. *J. Am. Chem. Soc.* **2006**, *128*, 2385.
(5) Kongkanand, A.; Tvrdy, K.; Takechi, K.; Kuno, M.; Kamat, P. V. *J. Am. Chem. Soc.* **2008**, *130*, 4007.
(6) Jiang, X.; Schaller, R. D.; Lee, S. B.; Pietryga, J. M.; Klimov, V. I.; Zakhidov, A. A. *J. Mater. Res.* **2007**, *22*, 2204.
(7) Samokhvalov, A.; Berfeld, M.; Lahav, M.; Naaman, R.; Rabani, E. *J. Phys. Chem. B* **2000**, *104*, 8631.
(8) Mamedov, A. A.; Belov, A.; Giersig, M.; Mamedova, N. N.; Kotov, N. A. *J. Am. Chem. Soc.* **2001**, *123*, 7738.
(9) Franzl, T.; Klar, T. A.; Schietinger, S.; Rogach, A. L.; Feldmann, J. *Nano Lett.* **2004**, *4*, 1599.
(10) Pacifico, J.; Jasieniak, J.; Gómez, D. E.; Mulvaney, P. *Small* **2006**, *2*, 199.
(11) Kagan, C. R.; Murray, C. B.; Nirmal, M.; Bawendi, M. G. *Phys. Rev. Lett.* **1996**, *76*, 1517.
(12) Crooker, S. A.; Hollingsworth, J. A.; Tretiak, S.; Klimov, V. I. *Phys. Rev. Lett.* **2002**, *89*, 186802.
(13) Franzl, T.; Shavel, A.; Rogach, A. L.; Gaponik, N.; Klar, T. A.; Eychmüller, A.; Feldmann, J. *Small* **2005**, *1*, 392.
(14) Weiss, E. A.; Porter, V. J.; Chiechi, R. C.; Geyer, S. M.; Bell, D. C.; Bawendi, M. G.; Whitesides, G. M. *J. Am. Chem. Soc.* **2008**, *130*, 83.
(15) Gross, D.; Susha, A. S.; Klar, T. A.; Da Como, E.; Rogach, A. L.; Feldmann, J. *Nano Lett.* **2008**, *8*, 1482.
(16) Aqua, T.; Cohen, H.; Vilan, A.; Naaman, R. *J. Phys. Chem. C* **2007**, *111*, 16313.
(17) Cohen, R.; Kronik, L.; Shanzer, A.; Cahen, D.; Liu, A.; Rosenwaks, Y.; Lorenz, J. K.; Ellis, A. B. *J. Am. Chem. Soc.* **1999**, *121*, 10545.
(18) Rei Vilar, M.; El Beghdadi, J.; Debontridder, F.; Artzi, R.; Naaman, R.; Ferraria, A. M.; Botelho do Rego, A. M. *Surf. Interface Anal.* **2005**, *37*, 673.
(19) Waldeck, D. H.; Alivisatos, A. P.; Harris, C. B. *Surf. Sci.* **1985**, *158*, 103.
(20) Gu, Y.; Waldeck, D. H. *J. Phys. Chem. B* **1998**, *102*, 9015.
(21) Salomon, A.; Cahen, D.; Lindsay, S.; Tomfohr, J.; Engelkes, V. B.; Frisbie, C. D. *Adv. Mater.* **2003**, *15*, 1881.

JP808803V